









Cite this: *Green Chem.*, 2020, **22**, 2947

Thermophilic bio-electro CO₂ recycling into organic compounds†

Laura Rovira-Alsina, ^a Elisabet Perona-Vico, ^b Lluís Bañeras, ^b
 Jesús Colprim, ^a M. Dolors Balaguer ^a and Sebastià Puig ^{*a}

Many industrial combustion processes produce carbon dioxide (CO₂) at high temperature, which may be electrically recycled into valuable chemicals using microorganisms as catalysts. However, little attention has been paid to handle the remaining heat of these processes as an alternative to increase CO₂ fixation and production rates. Thus, this study was aimed at steering electro bio-CO₂ recycling into organic compounds under thermophilic conditions. A mesophilic anaerobic sludge was adapted in lab-scale reactors at 50 °C, developing a resilient biocathode. High amounts of acetate (5250 mg L⁻¹) were accumulated during a long-term operation period (150 days). The maximum production rate was 28 g acetate per m² per d, with coulombic efficiencies over 80%. In terms of carbon (C) conversion, 0.31 kg of C as acetate were obtained per 1 kg of C as CO₂ inlet, with an energy demand of 24 kW h per 1 kg of acetate. *Thermoanaerobacterales* appeared to dominate the cathodic chambers, though they were compartmentalized by distinct bacterial communities in the electrode biofilm compared to the bulk liquid. This research delves into the sustained ability of a mixed microbial culture to electrochemically produce organic compounds at 50 °C and considers the possibility of using CO₂-saturated effluents from industrial heated point sources to bring the technology closer to its scale-up.

Received 25th January 2020,
 Accepted 31st March 2020

DOI: 10.1039/d0gc00320d
rsc.li/greenchem

1. Introduction

The continuous increase of atmospheric carbon dioxide (CO₂) due to anthropogenic activities as a relevant cause of climate change is out of debate.¹ Industrial combustion processes on a large scale, *i.e.* cement industries and refineries, largely contribute to this increase and are spread all over the globe. The emitted gases from these processes also alter the air temperature in the adjacent areas to the source, whose effects have not been exposed with enough relevance despite having a clear environmental impact. On the other hand, microbial electrochemical technologies (METs) have become a hotspot for the development of a versatile platform for the synthesis of fuels and chemical building blocks from CO₂,² thus partially contributing to mitigate its emissions. Applying an external voltage, hydrogen (H₂) and acetate can be simultaneously generated, using electricity as the only electron donor and CO₂ as the only

electron acceptor. Although acetate has a relatively low economic value, until now it has been the main soluble product obtained and it has been indispensable for chain elongation in secondary fermentation processes.³

The efficient conversion of electric energy into soluble products relies on the performance of catalysts, which can be biological or not. The use of microbial catalytic systems based on CO₂ capture and fixation allows for: (i) the production of CO₂-neutral commodities, (ii) versatile operation modes and (iii) minimizing the competition with food production for high-quality land.⁴ Among the main challenges of microbial catalysts, we should consider: (i) a limited rate and efficiency in the microbial reduction of CO₂ to multi-carbon compounds, (ii) an increased cost due to energy consumption for autotrophic growth, and (iii) an inadequate performance for industrial up-scaling and commercialization.⁴ Some of these bottlenecks can be overcome when working at higher temperatures. A greater reaction activity besides a larger bioavailability of soluble compounds can be achieved under thermophilic conditions (50–65 °C).⁵ Furthermore, the increase in temperature increases the reactions' kinetic constant value, diminishing the activation energy to reach the transition state. An elevated temperature may reduce the risk of microbial contamination, while pushing the proton mass transfer rate through the electrolyte.⁶ Besides, *in situ* product separation may be aided, as intense heat triggers the volatility of organic compounds,

^aLEQUiA. Institute of the Environment, University of Girona. Campus Montilivi, C/Maria Aurèlia Capmany, 69, E-17003 GironaCatalonia, Spain.
 E-mail: sebastia.puig@udg.edu

^bgEMM. Group of Molecular Microbial Ecology. Institute of Aquatic Ecology, University of Girona. Campus Montilivi, C/Maria Aurèlia Capmany, 69, E-17003 GironaCatalonia, Spain

† Electronic supplementary information (ESI) available. See DOI: 10.1039/d0gc00320d



which alleviates the need for additional energy input and further recovery steps.⁷ High temperatures will also reduce the solubility of gases, which will cause a two-side effect. On the one hand, less oxygen will be dissolved in solution, which is advantageous for anaerobic microorganisms. On the other hand, H₂ and CO₂ solubility will be reduced as well, which limits carbon and energy availability for biotic reactions. In consideration of the foregoing, operational management becomes more difficult and many sensors, electrodes and membranes may not be suitable because of their limited temperature range.⁸

Until now, microbial electrosynthesis under thermophilic conditions has been rarely studied, though potential applications would not only reevaluate industrial off-gases but also boost the product separation procedure. The recent advances and range of possibilities for thermophilic microorganisms in METs were first reviewed by Dopson *et al.* (2016)⁴⁰ and recently by Shrestha *et al.* (2018).⁸ Initial studies confirmed H₂ production at 55 °C by a *Firmicutes* population.⁹ Later, Faraghiparapari and Zengler (2017)²² determined the optimal temperature range for acetate generation using two different *Moorella* strains, whereas Yu and colleagues studied the enhancement of applying immobilized cathodes for simultaneous acetate and formate production.⁴ Thermophilic methane (CH₄) production has also been examined by different authors,^{10,11} and the interaction between methanogens and acetogens has been recently explained comparing the microbial communities before and after electricity supply.¹² Regardless of the examples provided above, intensive research on thermophilic METs is lacking in order to evaluate their implementation in comparison with other equivalent technologies for the effective conversion of CO₂ streams generated from thermal industrial processes. In this regard, the purpose of the present work was to unveil the key operational conditions for the thermophilic bio-electro CO₂ recycling into organic compounds and investigate the key limiting factors to enhance high production rates in the long-term.

2. Materials and methods

2.1. Setup. Bioreactor construction and operational conditions

Two H-type METs (Pyrex V-65231 Scharlab, Spain) were constructed (named HT1, HT2) using two identical glass bottles of 0.25 L, separated by a cation exchange membrane (2×10^{-4} m²) (standard CMX Neosepta, Tokuyama Corp., Japan). The cathode consisted of a plain carbon cloth (Thickness 490 μm; NuVant's Elat LT2400 FuelCellsEtc, USA) of 15 cm² (working area of 30 cm²) connected to a stainless steel wire, while the anode was a graphite rod (EnViro-cell, Germany). The anode electrode was replaced every 8 weeks to maintain a stable cell potential. An Ag/AgCl electrode (+0.197 V vs. SHE, model RE-5B, BASI, UK) with an operating temperature range from 0 to 60 °C was placed in the cathode chamber and used as the reference electrode. Reactors were sealed with butyl rubber

caps to prevent gas leakage and were operated in a three-electrode configuration with a potentiostat (BioLogic, Model VSP, France), which controlled the cathode potential at -0.6 V vs. SHE and monitored the current demand. All the potentials reported in this work are relative to the standard hydrogen electrode (SHE) unless otherwise noted. To validate the reproducibility of the process, two extra reactors (HT3, HT4) were constructed using the same configuration and materials, but they were started up with a mixture of HT1 and HT2 effluents after 67 days since inoculation. All systems were operated in batch mode and kept in the dark to avoid the growth of phototrophic microorganisms. The temperature was kept constant at 50 °C either by using an orbital incubator (SI600 Stuart, UK) or externally jacketed reactors (PolyScience, Illinois), and an agitation speed of 80 rpm was fixed (SB 161 Stuart, UK) to enable mixing and facilitate mass transfer inside the cathode chambers.

2.2. Inoculum and growth media

A sample from an anaerobic digester working at 37.5 °C of Girona's wastewater treatment plant (WWTP) located in Spain was used as an inoculum. A 1 : 20 dilution was first incubated in two fermentative reactors to promote acetogenesis. During this enrichment stage, 2-bromoethanesulfonic acid (10 mM) was added to prevent methanogenesis.¹³ After 30 days, 864 ± 17 mg L⁻¹ of acetate had been accumulated, with a maximum production rate of 0.65 mg acetate per mg SSV per d. For the inoculation of the two microbial electrolysis cells (HT1 and HT2), the anaerobic sludge was again diluted 20 times with ATCC1754 PETC medium reformulated to remove all sources of organic carbon (Table 1, ESI†). pH was initially adjusted to 6.0 using NaOH 5.0 M and a methanogen inhibitor was added punctually during the first month. After 67 days of operation, two similar reactors (HT3 and HT4) were inoculated with 18% of the previous ones, 5% of the initial fermentative reactor and 77% of fresh medium (all percentages referred to v/v). Table 2 (ESI)† describes in more detail the operational conditions and inoculation source for each reactor.

2.3. Electrochemical characterization

Preliminary tests were performed in microbial electrolysis cells (MECs) under open/closed circuit and abiotic conditions at different temperatures (25 °C, 37 °C and 50 °C), while the inoculum activity was tested in batch fermentation using 0.1 L penicillin bottles sealed with butyl rubber stoppers and aluminium crimp caps. Software from BioLogic (EC-Lab v10.37) was used to run simultaneous multitechnique electrochemistry routines with a potentiostat, which included chronoamperometry (CA), open circuit voltage (OCV) and cyclic voltammetry (CV). A cathode potential of -0.6 V was fixed for CA whereas its variation was followed during OCV. CV under turnover conditions (in the presence of an electron acceptor) was performed before and after inoculation to qualitatively distinguish between biotic and abiotic performances. Four cycles from -0.2 V to -1 V were performed by imposing a linear scanning potential rate of 1 mV s⁻¹. To represent the results, the



last cycle of every CV is shown. Prior to use, the working electrodes were pre-treated in a 0.5 M solution of HCl and a 0.5 M solution of NaOH for a total of two days, and rinsed with de-ionized water for an additional day. At the end of the experimental study, the voltage of the reference electrodes was measured to check for any shift that may have occurred during operation.

2.4. Analytical methods and calculations

Samples from the liquid phase were taken twice a week. To maintain a constant chamber volume of 0.22 L, withdrawn liquid during sampling was replaced with freshly prepared medium saturated with CO₂. Measurements for conductivity and pH were performed with an electric conductivity meter (EC-meter basic 30+, Crison, Spain) and a multimeter (MultiMeter 44, Crison, Spain), respectively, which were calibrated to analyse at 50 °C. The concentration of organic compounds (volatile fatty acids and alcohols) in the liquid phase was assessed using an Agilent 7890A gas chromatograph equipped with a DB-FFAP column and a flame ionization detector.

A mixture of CO₂ and H₂ (20 : 80 v/v) (Praxair, Spain) was bubbled into the fermenters, while pure CO₂ (99.9%, Praxair, Spain) was used to feed the four MECs. Gas was sparged for 10 minutes in the cathode chamber every 2–3 days. To quantify gas production in the MECs, the pressure in the headspace of the reactors was measured using a digital pressure sensor (differential pressure gauge, Testo 512, Spain) and gas samples were analysed periodically during experiments by gas chromatography (490 Micro GC system, Agilent Technologies, US). The GC was equipped with two columns: a CP-molesive 5A for CH₄, carbon monoxide (CO), H₂, oxygen (O₂) and nitrogen (N₂) analysis, and a CP-Poraplot U for CO₂ analysis. Both columns were connected to a thermal conductivity detector (TCD).

The concentration of dissolved H₂ and CO₂ in the liquid media was calculated using Henry's law at 50 °C (eqn (1)), where C_i is the solubility of a gas in a particular solvent (mol L⁻¹), H_i is Henry's law constant in mol L⁻¹ atm⁻¹ (0.0007 for H₂ and 0.0195 for CO₂) and $P_{\text{gas } i}$ is the partial pressure of the gas in atm.

$$C_i = H_i P_{\text{gas},i} \quad (1)$$

The coulombic efficiency (CE) for the conversion of current into products was calculated according to the study by Patil *et al.* (2015)⁴¹ (eqn (2)). C_i is the compound i concentration in the liquid phase (mol L⁻¹), n_i is the molar conversion factor (2 and 8 eq. mol⁻¹ for H₂ and acetate, respectively), F is Faraday's constant (96 485 C mol e⁻¹), V_{NCC} is the net liquid volume of the cathode compartment (L), and I is the intensity demand of the system (A).

$$\text{CE}(\%) = \frac{C_i \cdot \sum_i n_i \cdot F \cdot V_{\text{NCC}}}{\int_0^t I \cdot dt} \times 100 \quad (2)$$

Carbon conversion efficiency (CCE) was calculated as the percent variation between the initial and final samples in a

batch as stated in eqn (3). ΔC_{CO_2} is the difference of CO₂ in the gas plus liquid phases from the beginning (immediately after feeding the system) to the end of a batch, and $\Delta C_{\text{products}}$ is the difference of organic products (*i.e.* acetate) between batches.

$$\text{CCE}(\%) = \frac{\Delta C_{\text{CO}_2} - \Delta C_{\text{products}}}{C_{\text{CO}_2 \text{ initial}}} \times 100 \quad (3)$$

2.5. Extraction of DNA and microbial community structure determination

Samples of carbon cloth and bulk liquid for each reactor were taken at different operation times to assess the microbial community composition. Samples were extracted at 133 and 228 days of operation for HT1, 152 and 228 for HT2, 84 and 160 for HT3 and 65 and 160 for HT4. Before DNA extraction, bulk liquid cells were pelleted by centrifugation, whereas carbon cloth samples were used directly. DNA was extracted using a FastDNA® SPIN kit for Soils (MP Biomedicals, USA) following the manufacturer's instructions. The extracts were distributed in aliquots and stored at -20 °C, and the DNA concentration was measured using a Nanodrop™ 1000 spectrophotometer (Thermo Fisher Scientific, USA). The quality of DNA extracts for downstream molecular applications was checked after PCR detection of 16S rRNA using the universal bacterial primers 27F and 1492R.

The hypervariable V4 region of the 16S rRNA gene was amplified using the primers 515F and 806R following the method described by Kozich and Schloss, which was adapted to produce dual-indexed Illumina compatible libraries in a single PCR step.¹⁴ First, PCR was performed using fusion primers with target-specific portions¹⁵ and Fluidigm CS oligos at their 5' ends. Second, PCR targeting the CS oligos was used to add sequences necessary for Illumina sequencing and unique indexes. PCR products were normalized using Invitrogen SequalPrep DNA normalization plates and the pooled samples were sequenced using an Illumina MiSeq flow cell (v2) in a 500-cycle reagent kit (2 × 250 bp paired-end reads). Finally, sequencing was performed at the RTSF Core facilities at the Michigan State University USA (<https://rtsf.natsci.msu.edu/>).

Sequences were filtered for minimum length (>250 nt) and maximum expected errors (<0.25). Paired-end sequences were merged, quality filtered and clustered into OTUs (operational taxonomic units) using USEARCH v9.1.13.¹⁶ They were clustered at the 97% identity using UCLUST,¹⁷ and checked for the presence of chimeras. OTUs containing only one sequence (singletons) were removed. The subsequent analyses were performed with Qiime v1.9.1.¹⁸ Representative OTU sequences were aligned using PyNAST with default parameters against Silva 132 release (April 2018). The same reference database was used to taxonomically classify the representative sequences using UCLUST. Direct BLASTn searches at the NCBI of selected sequences were used when poor identifications with the Silva database were obtained. Sequences presented in this study have been submitted to the GenBank database within the SRA accession number PRJNA557160.



Samples from the reactors' cathode HT1–2 and HT3–4 were taken for SEM imaging after 228 and 160 days of operation, respectively. They were immersed in a 0.1 M cacodylate buffer solution at pH 7.4 with 2.5% (w/v) glutaraldehyde for 4 hours. After immersion, they were washed twice with cacodylate buffer and water, and dehydrated in an ethanol series. Dehydration with graded ethanol followed the temperature steps of 50, 75, 80, 90, 95 and 3 times 100 °C in periods of 20 minutes. The fixed samples were dried with a critical point dryer (model K-850 CPD, Emitech, Germany) and sputtered-coated with a 40 nm gold layer. The coated samples were examined with a SEM (model DSM-960; Zeiss, Germany) at 20 kV. Images were captured digitally using ESPRIT 1.9 BRUKER software (AXS Microanalysis GmbH, Germany). All analyses were performed in the *Serveis Tècnics de Recerca (STR)* at the University of Girona.

3. Results and discussion

3.1. Selection of the operational conditions to reinforce hydrogen production

The effect of cathode potential and temperature on electrochemical H₂ production and energy consumption was first assessed in duplicate to fix optimal working conditions in the H-type reactors. Regarding temperature, the cathode potential was set at –0.8 V, and electrochemical H₂ production was then studied in terms of volumetric load and electric energy consumption (Fig. 1A). The relationship between both parameters for each temperature was found to be linear (R^2 between 0.995 and 1), as other studies also pointed out.¹⁹ The H₂ production rate per unit of energy consumed was higher at 50 °C (218 m³ H₂ per m³ NCC per d) in contrast to that at 37 or 25 °C (124 and 80 m³ H₂ per m³ NCC per d, respectively). Similarly, Chris Van de Goor and co-workers concluded that higher temperatures positively influenced the hydrogen evolution reaction on platinum electrodes by decreasing the overpotential and modifying the activation energy.²⁰

The H₂ production rate at 50 °C was also tested at different potentials in terms of volumetric load and electric energy consumption (Fig. 1B). The results showed a linear correlation between H₂ production and energy consumption (R^2 between 0.982 and 0.997). Higher H₂ production for the same energy consumption was obtained when the cathode potential was fixed at less negative values, in agreement with previous studies.²¹ At –0.4 V, almost no production was observed. At –0.6 V instead, H₂ generation was slower but more electrically efficient compared to that at –0.8 V.

According to the results, the conditions were set as 50 °C and –0.6 V in subsequent experiments to produce H₂ as reducing power for acetate generation. However, a wider temperature and potential range screening could give insight into the most appropriate configuration.

3.2. Long-term operation of thermophilic METs

The start-up time of MEC reactors was reduced to 10 days (Fig. 2) and after 150 days of operation, the accumulated acetic

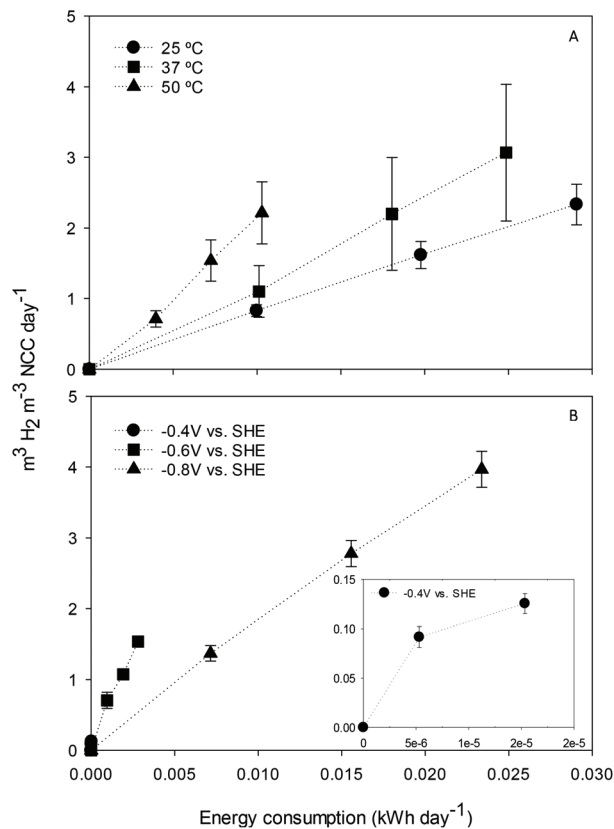


Fig. 1 Electrochemical hydrogen production over electric energy consumption at –0.8 V and different temperatures (A), or 50 °C and different poised cathode potentials (B). The error bars represent the deviation between the two reactors tested.

acid concentration reached 3640 ± 1200 mg L⁻¹ on average, with a maximum production rate of 286 ± 126 mmol acetate per m² per d. Specifically, HT3 achieved the highest concentration and production rate, with a maximum titer of 5250 mg L⁻¹ and 468 mmol acetate per m² per d, respectively.

The number of studies focusing on the bioelectrochemical synthesis of acetate under thermophilic conditions is scarce (Table 3, ESI).[†] Using electricity and CO₂ as the sole carbon source to feed *Moorella thermoautotrophica* at 50 °C, Yu and co-workers achieved an acetate production rate of 58.19 mmol m⁻² d⁻¹.⁴ However, a different study working with the same strain at 60 °C obtained a much lower rate, 3.5 ± 0.3 mmol m⁻² d⁻¹.²² Recently, Song *et al.* (2019b)¹² continuously purged CO₂ with a gas diffuser into a membrane-less reactor. This configuration decreased the internal resistance, which may have helped to obtain a higher acetate titer compared to the present work (10 500 mg L⁻¹). However, at a similar fixed potential (–0.65 V), the maximum product formation velocity was lower (160 mmol acetate per m² per d). One of the main challenges in MEC research is to know how to maintain microbial activity for sustained long-term production.²³ The mixed community of this study could remain active for a long time period (>150 days), which is a reasonable time span to consider thermophilic systems as a reliable oper-



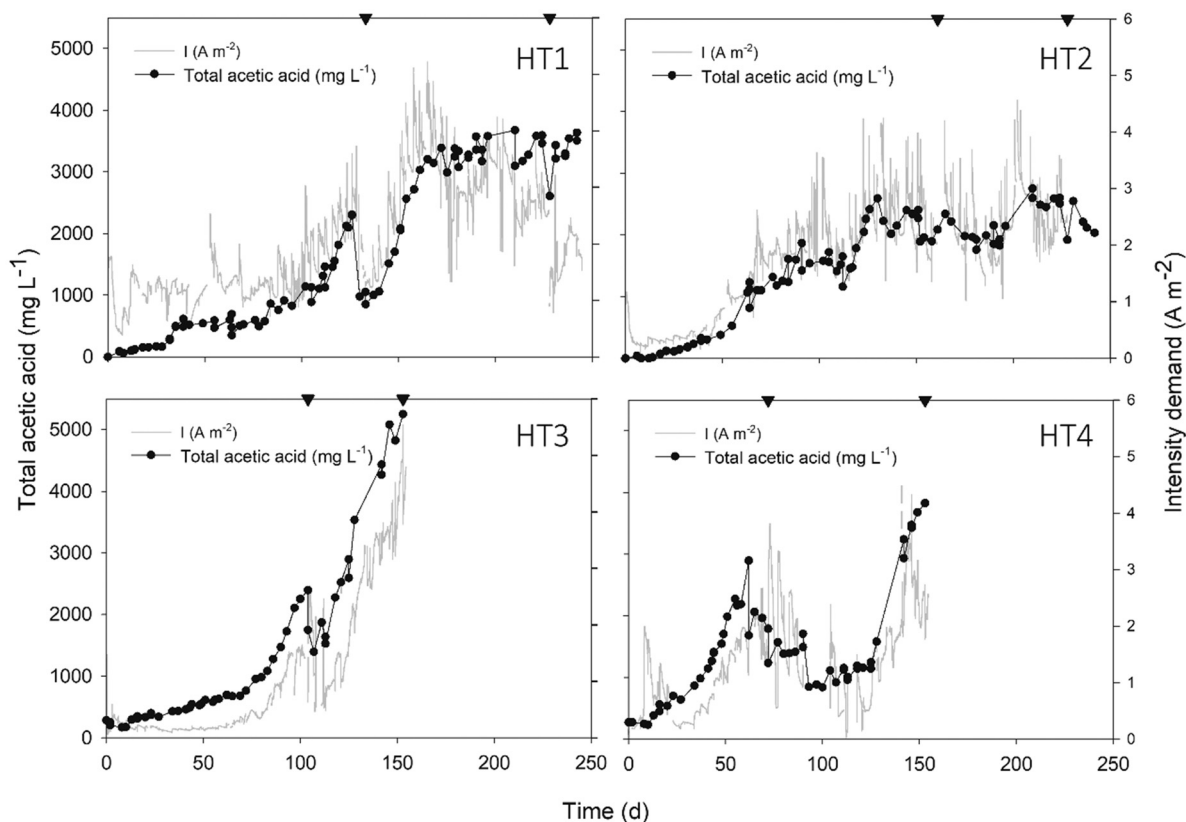


Fig. 2 Total acetic acid concentration (anode + cathode in mg L^{-1}) and intensity demand profiles (A m^{-2}) over time in four different reactors. Acetic acid concentration in the anodic chamber accounted for 20% of the total amount. Sampling points for DNA extraction are indicated by inverted triangles and CO_2 was sparged to feed the system every time a sample was taken.

ation in MEC development. This, together with the fact that biofilms grown at higher temperatures are more electro-chemically active than those grown at lower temperatures,²⁴ is a key starting point to encourage active research in thermophilic METs.

Intensity demand seemed to be related to acetic acid concentration, as the same profiles were observed during the overall study (Fig. 2). This might be explained because as acetate was being accumulated over time, the liquid conductivity increased (see Fig. 1, ESI†) and thus, the internal resistance of the bulk liquid diminished. According to Ohm's law and considering a stable cell potential ($E_{\text{cell}}: -3.1 \pm 0.1$, data not shown), the intensity demand was consequently increased.

More than 80% of the electrons were recovered in the form of H_2 and acetate (Fig. 3). The remaining 20% could be attributed to energy consumed for cell maintenance, oxygen scavenging, or simply lost in the system.²⁵ H_2 mainly explained the whole consumption, while acetate varied depending on the exponential period since part of it could be consumed to fermentatively produce other substances. CH_4 and CO were present in trace amounts ($<0.003\%$ v/v). Ethanol was detected transiently at concentrations below 160 mg L^{-1} , whereas butyric, valeric and propionic acids were found in minor amounts ($<50 \text{ mg L}^{-1}$). On average, one-fourth of the total energy consumed ($24 \pm 8 \text{ kW h}$) was destined to obtain 1 kg of

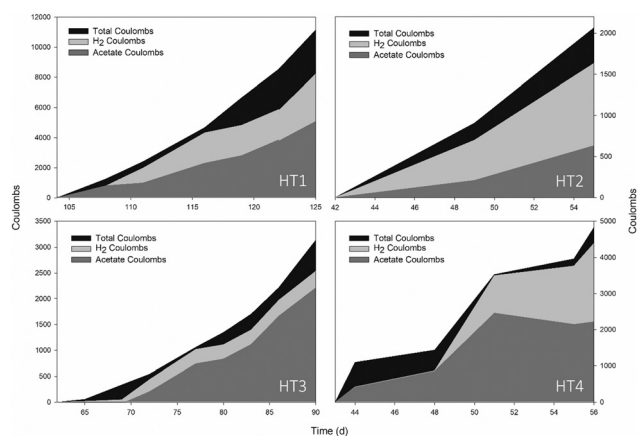


Fig. 3 Distribution of the accumulated coulombs in products compared to total coulombs consumed over time in each reactor. Different intervals have been taken corresponding to the first producing period of each reactor.

acetate while the rest was used for the generation of 1 kg of H_2 ($80 \pm 5 \text{ kW h}$).

CCE fluctuated over time and differed for every feeding interval. Considering that every batch was initiated with approximately 12 mmol of CO_2 (sum of gas and liquid phases),



an average CCE of $45 \pm 16\%$ was obtained for the same producing periods shown in Fig. 3. It means that from the inlet, half of the CO_2 was converted into products, giving an associated carbon ratio from CO_2 to product of 2.22 ± 0.79 mmol C_{CO_2} : mmol $\text{C}_{\text{product}}$ (0.31 ± 0.86 kg of product per kg of CO_2 consumed). A different study for the production of bioplastics obtained a CCE of 73%, in which 0.41 kg of carbon in the form of PHA were generated for every kg of applied carbon as CO_2 .²⁶ The values of the present work are lower, but it must be considered that CO_2 was less available, since the solubility of gases diminishes with increasing temperature. However, with the given data of other thermophilic studies, they cannot be compared to similar systems catalysing comparable end-products. Nevertheless, the low CO_2 solubility at high temperature could be reinforced by using gas diffusion electrodes that enhance mass transport and increase the CCE.³⁹

3.3. Contribution of biofilms to net H_2 production

Elucidating the different operational parameters in METs can give insight into how to steer the system performance. H_2 has been postulated to act as a mediator in redox reactions.¹ Hence, a test to differentiate biotic from pure electrochemical H_2 evolution in the studied MECs was carried out. For this, individual batches considering the time between feeding events were used. The production rate was calculated in each reactor taking into account the H_2 accumulated in the gas plus liquid phases after 4.5 hours. The biotic production was then differentiated from the abiotic considering the H_2 production of the control (Fig. 2a, ESI^\dagger) under the same conditions regarding potential (-0.6 V) and temperature (50 °C) (see section 3.1). Furthermore, to quantify the total bio H_2 formation, the stoichiometric H_2 needed to generate the detected acetate during the same period also had to be considered (Fig. 2c, ESI^\dagger).

During control tests, an abiotic molar rate of 0.77 ± 0.61 mol H_2 per m^2 per d was obtained. This value increased up to 1.25 ± 0.38 mol H_2 per m^2 per d once the reactors were inoculated, and to 8.18 ± 1.51 mol H_2 per m^2 per d when stoichiometric H_2 consumed for acetate generation was contemplated. This means that H_2 production was 10-fold higher in biotic reactors than in the abiotic ones, representing 90.59% of the total production. These values were one order of magnitude above those obtained in other thermophilic studies⁹ even at a less negative fixed potential. They were still low in contrast to those of Ni-based catalysts, although they were similar to those reported in studies that had used stainless steel electrodes.²⁷

Cyclic voltammetry (CV) was performed for abiotic (prior to inoculation) and biotic (42 days after inoculation) conditions, which clearly distinguished the microorganisms' activity (Fig. 4A). With a similar pH (5.86 vs. 5.81, respectively), the intensity demand curve of the biotic system reached 47.5 mA, which compared to the non-inoculated one (8.20 mA) was an indicator of an increase in H_2 production. The presence of redox-active components could not be confirmed in the catho-

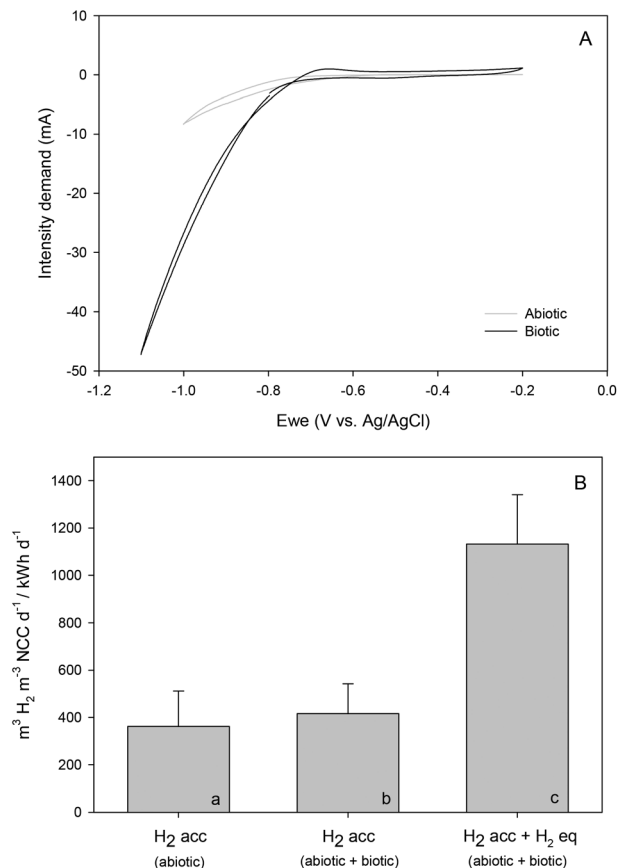


Fig. 4 Comparison between the abiotic and biotic reactors during cyclic voltammetry (A) and H_2 production over the electrical energy consumption test (B) at 50 °C. A distinction has been made between the H_2 accumulation (H_2 acc) in the gas plus liquid phases (a and b) and the H_2 equivalent (H_2 eq.) produced regarding organics concentration in the liquid phase (c).

lyte when microorganisms were not present, with the onset potential of H_2 evolution at around -0.8 V vs. Ag/AgCl.

Meanwhile, a shift to a slightly higher potential of -0.7 V vs. Ag/AgCl was observed when the reaction was bio-catalysed, evidencing hydrogen-mediated production of commodity chemicals.²⁸ These results are clearly shown in Fig. 4B, where the volumetric H_2 rate as a function of electrical energy consumption under abiotic and biotic conditions differed by 70% when considering equivalent H_2 for organics production. The possible role of an enriched electro-synthetic community was also highlighted by other researchers such as LaBelle and co-workers, which was found to lower the H_2 evolution overpotential by 0.25 V.²⁹

3.4. Effects of partial medium replacement on inhibitory mechanisms and acetate productivity

It is well known that regular addition of nutrients into the bulk liquid is necessary to maintain good organic production rates.³⁰ Partial medium replacement has an additional advantage compared to nutrient amendment, which is the dilution of potential inhibitors that may have accumulated during oper-



Table 1 Acetate concentration, production rate, undissociated acetic acid content (HAc), coulombic efficiency (CE), pH and electric conductivity (EC) before and after medium replacement during specific periods in each of the four reactors

Reactor	Before							After						
	Days	Acetate (mM)	Prod. rate (mmol m ⁻² d ⁻¹)	HAc (mM)	CE (%)	pH	EC (mS cm ⁻²)	Days	Acetate (mM)	Prod. rate (mmol m ⁻² d ⁻¹)	HAc (mM)	CE (%)	pH	EC (mS cm ⁻²)
HT1	95–105	19.30	37.00	1.08	54.49	5.74	4.39	105–112	18.00	100.49	0.46	83.09	5.88	10.68
HT2	95–112	27.91	7.90	9.18	30.45	5.53	3.83	112–130	25.95	97.29	3.18	59.53	5.62	9.91
HT3	168–181	65.12	20.18	7.80	12.84	4.83	7.66	183–195	58.22	168.51	7.96	40.17	4.99	6.89
HT4	170–181	49.51	43.15	16.35	30.25	5.21	6.8	183–195	41.50	204.33	2.78	47.78	6.02	8.7

ation. For instance, the accumulation of organic acids and their undissociated forms has been demonstrated to inhibit the metabolic activity of homoacetogens.³¹ In the four thermophilic MECs, we tested the effect of accumulated undissociated acetic acid (HAc) on productivity by substituting part of the cathode compartment with fresh medium in different tests (following the order of reactors, from 15 to 35%).

Every time a part of the medium was replaced, the product formation velocity increased (Table 1). Undissociated HAc seemed to have a minor effect in our systems although estimated concentrations were found in inhibition ranges for homoacetogenic bacteria.³² For instance, similar HAc values before and after medium replacement resulted in an 8-fold increase of acetate production rates in HT3. In other cases, greater productions were found at higher HAc concentrations, (*i.e.* HT4 *vs.* HT1). A second explanation for the observed results was in line with the depletion of an essential component of the medium during batch experiments. In all reactors, acetate production rates increased significantly after medium replacement. The enhancement ranged from roughly 3 times (from 37 to 100 mmol m⁻² d⁻¹ in HT1), to more than 10 times (from 8 to 97 mmol m⁻² d⁻¹ in HT2). In all cases, increments in production rates were concomitant to higher CE. Differently, the substrate (CO₂) was periodically fed during the whole study and it was never entirely consumed, so carbon depletion could also be excluded as a potential factor explaining changes in acetate production.

Further investigation should be focused on the effect of macro and micronutrient depletion as well as the possible excreted inhibitor accumulation.

3.5. Microbial community analysis

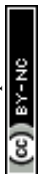
At the end of experiments, bacterial cells firmly attached to the cathode surface were clearly visualized in SEM images (Fig. 3, ESI†). Cells appeared to be embedded in a complex matrix, poorly structured in layers, and partly surrounded by tiny particles, most likely ensuring an intimate contact with the electrode surface. The microbial community structure in the four MECs was analysed by barcoded amplicon sequencing of the 16S rRNA gene. Microbial communities in the four reactors were dominated by *Firmicutes* bacteria, accounting for 85–94% in the biofilm and 65–69% in the bulk liquid (Fig. 5). *Proteobacteria* was also present, being more abundant in bulk liquid (26–28%) compared to the biofilm (13–4%). The thermophilic community in both sample types was composed of

the orders *Thermoanaerobacterales*, *Betaproteobacteriales* and *Clostridiales*, the former being the predominant according to relative number of sequences. No methanogenic archaea could be detected in the systems. At the genus level, *Moorella*, *Caloribacterium*, *Desulfotomaculum* and *Tepidiphilus* were the most representative, but at different relative abundances between samples (Fig. 5). Further analysis using BLASTn searches revealed that biocathodes were mainly dominated by *Moorella perchloratireducens* strain An10 (NR 125518.1, 99% sequence similarity) and *Caloribacterium cisternae* strain GL43 (NR 118109.1, 96% sequence similarity).

These results agree with previous analyses of a thermophilic biocathode for H₂ production.⁹ *Moorella thermoacetica* and *M. thermoautotrophica* have been described as electro-trophic microorganisms and have been shown to be able to reduce CO₂ to acetate in a wide temperature range (from 25 to 70 °C) in bioelectrochemical systems.²² The sequences found in our systems were more closely related to *M. perchloratireducens* but its putative participation in the electron harvesting process is not known. Except for HT3, relative abundances of *Moorella* related sequences remained at similar values both in liquid and biofilm samples and were sustained through time, posing a reasonable doubt on the participation of this bacterium in electron harvesting in our systems.

In contrast, *Desulfotomaculum* species are considered sulfate-reducing bacteria (SRB). In our systems, they were mainly present in bulk samples and they could probably use sulfate as a terminal electron acceptor to produce reduced hydrogen sulfide (H₂S) when organic substrates were available, but also use CO₂ as the sole carbon source.¹² However, very low amounts of H₂S were found in the liquid media (0.021 ± 0.005 mg L⁻¹). Instead, in CO₂ converting bioelectrochemical systems, SRB such as *Desulfovibrio* and *Desulfobacterium* have been proposed as H₂ producers, electron transfer enhancers and acetate producers.^{33–35} Moreover, they can putatively reduce acetic and butyric acids to the corresponding alcohols or ketones.¹

Differently, in thermophilic microbial fuel cells, Wrighton and co-workers demonstrated the predominance of *Firmicutes* (>50%) in a bioanode community. Those bacteria were electricity-producing members, which used acetate as a carbon source. *Moorella* and *Desulfotomaculum* related sequences were identified as presumably responsible for anode electroactive reactions.³⁶ Similarly, *Caloribacterium* species have been found on bio-anodes, suggesting its participation in electron



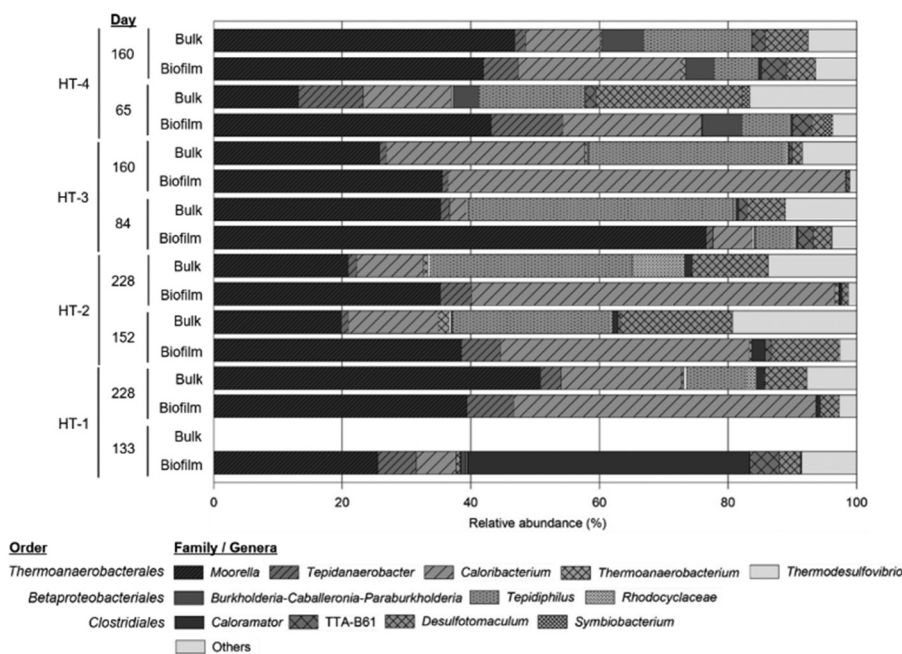


Fig. 5 Microbial community composition in biofilm and bulk liquid samples. The bar chart shows relative abundances of main genera (or families when no further classification could be obtained). Sampling days for each reactor (named HT1–4) are indicated.

transfer.³⁷ In a thermophilic bioreactor, enriched microbial communities revealed a high abundance of both, *Caloribacterium* and *Desulfotomaculum* species when feeding with a synthetic syngas mixture or CO alone. It was proposed that these thermophiles converted the input gas mainly to H₂ and acetate.³⁸

In the mature biofilm (>150 days of constant operation) collected from three out of the four systems analysed in this work, the relative abundance of *Caloribacterium* was higher compared to previous samples. This confirms a selective enrichment of this bacteria on the cathode surface. The latter, together with sustained H₂ evolution and acetate production, suggests the participation of *Caloribacterium* in electrode harvesting. If this could be confirmed by additional experimentation using purified *Caloribacterium* isolates, it would be an additional example of a single species putatively acting as an electro-troph and electrogenic bacterium.

4. Conclusions

This study has reported on the lasting ability of a mixed microbial culture to effectively produce sustained H₂ and acetate under thermophilic conditions. Our results show a reasonable resilience and robustness of the process for a period of over 150 days. An equivalent H₂ formation rate of 8.2 mol H₂ per m² per d was obtained, which exceeded 10 times the abiotic production under the same conditions. Intensity demand profiles were concomitant with acetate generation, providing the power dependence of the system. Approximately, 85% of the electrons consumed were recovered

into products, whose production was resumed in new set-ups shortly after inoculation or medium replacement, indicating a high stability of the microbial community. Micronutrients and enzyme cofactors, but no inhibitory wastes such as accumulated undissociated acids, seemed to have a significant effect on acetate production as observed after repetitive partial replacements of the cathodic electrolyte. Considering the changes of biofilm and bulk liquid microbiomes, the anaerobic sludge from a conventional WWTP turned out to be a suitable inoculum source for thermophilic MEC reactors. *Moorella* and *Caloribacterium* related sequences were found to be the most abundant in the cathode biofilms of the four systems. The obtained results propel research interest to promote the suitable working parameters to obtain higher valuable compounds and fully optimise the performance by integrating carbon capture and utilisation units and replace the required energy for renewable resources.

Conflicts of interest

The authors report no conflicts to declare. The authors alone are responsible for the content and writing of this article.

Acknowledgements

This study has received funding from the European Union's Horizon 2020 research and innovation program under the grant agreement no. 760431. L. R.-A. acknowledges the support from the Catalan Government (2018 FI-B 00347) in the



European FSE program (CCI 2014ES05SFOP007). E. P.-V. is grateful for the Research Training grant from the University of Girona (IFUDG2018/52). S. P. is a Serra Húnter Fellow (UdG-AG-575) and acknowledges the funding from the ICREA Acadèmia award. LEQUIA and IEA have been both recognized as consolidated research groups by the Catalan Government (2017-SGR-1552 and 2017-SGR-548).

References

- Z. J. Ren, X. Huang, H. D. May, L. Lu, Y. Jiang and P. Liang, *Water Res.*, 2019, **149**, 42–55.
- Y. Zhang and I. Angelidaki, *Water Res.*, 2014, **56**, 11–25.
- C. M. Spirito, H. Richter, K. Rabaey, A. J. M. Stams and L. T. Angenent, *Curr. Opin. Biotechnol.*, 2014, **27**, 115–122.
- L. Yu, Y. Yuan, J. Tang and S. Zhou, *Bioelectrochemistry*, 2017, **117**, 23–28.
- B. K. Chaudhary, Final degree thesis, Asian Institute of Technology, 2008.
- A. Hussain, P. Mehta, V. Raghavan, H. Wang, S. R. Guiot and B. Tartakovsky, *Enzyme Microb. Technol.*, 2012, **51**(3), 163–170.
- D. R. Lovley and K. P. Nevin, *Curr. Opin. Biotechnol.*, 2013, **24**(3), 385–390.
- N. Shrestha, G. Chilkoor, B. Vemuri, N. Rathinam, R. K. Sani and V. Gadhamshetty, *Bioresour. Technol.*, 2018, **255**, 318–330.
- Q. Fu, H. Kobayashi, Y. Kuramochi, J. Xu, T. Wakayama, H. Maeda and K. Sato, *Int. J. Hydrogen Energy*, 2013, **38**(35), 15638–15645.
- Q. Fu, Y. Kuramochi, N. Fukushima, H. Maeda, K. Sato and H. Kobayashi, *Environ. Sci. Technol.*, 2015, **49**(2), 1225–1232.
- H.-Y. Yang, B.-L. Bao, J. Liu, Y. Qin, Y.-R. Wang, K.-Z. Su, J.-C. Han and Y. Mu, *Bioelectrochemistry*, 2017, **119**, 180–188.
- H. Song, O. Choi, A. Pandey, Y. G. Kim, J. S. Joo and B.-I. Sang, *Bioresour. Technol.*, 2019, **281**, 474–479.
- D. A. Jadhav, A. D. Chendake, A. Schievano and D. Pant, *Bioresour. Technol.*, 2018, **277**, 148–156.
- J. J. Kozich, S. L. Westcott, N. T. Baxter, S. K. Highlander and P. D. Schloss, *Appl. Environ. Microbiol.*, 2013, **79**(17), 12–20.
- T. Stoeck, D. Bass, M. Nebel, R. Christen, M. D. M. Jones, H.-W. Breiner and T.-A. Richards, *Mol. Ecol.*, 2010, **19**(Suppl 1), 21–31.
- R. C. Edgar and H. Flyvbjerg, *Bioinformatics*, 2015, **31**(21), 3476–3482.
- R. C. Edgar, *Bioinformatics*, 2010, **26**(19), 2460–2461.
- J. G. Caporaso, K. Bittinger, F. D. Bushman, T. Z. DeSantis, G. L. Andersen and R. Knight, *Bioinformatics*, 2010, **26**(2), 266–267.
- P. Batlle-Vilanova, S. Puig, R. Gonzalez-Olmos, A. Vilajeliu-Pons, L. Bañeras, M. D. Balaguer and J. Colprim, *Int. J. Hydrogen Energy*, 2014, **39**(3), 1297–1305.
- C. Van De Goor, Z. Li and G. Mul, Final degree thesis, University of Twente, 2016.
- J. S. Geelhoed and A. J. M. Stams, *Environ. Sci. Technol.*, 2011, **45**(2), 815–820.
- N. Faraghiparapari and K. Zengler, *J. Chem. Technol. Biotechnol.*, 2017, **92**(2), 375–381.
- S. M. T. Raes, L. Jourdin, C. J. N. Buisman and D. P. B. T. B. Strik, *ChemElectroChem*, 2017, **4**(2), 386–395.
- S. A. Patil, F. Harnisch, B. Kapadnis and U. Schröder, *Biosens. Bioelectron.*, 2010, **26**(2), 803–808.
- P. Batlle-Vilanova, R. Ganigue, S. Ramió-Pujol, L. Bañeras, G. Jiménez, M. Hidalgo, M. D. Balaguer, J. Colprim and S. Puig, *Bioelectrochemistry*, 2017, **117**, 57–64.
- T. P. Sciarria, P. Batlle-Vilanova, B. Colombo, B. Scaglia, M. D. Balaguer, J. Colprim, S. Puig and F. Adani, *Green Chem.*, 2018, **20**(17), 4058–4066.
- A. Kundu, J. N. Sahu, G. Redzwan and M. A. Hashim, *Int. J. Hydrogen Energy*, 2013, **38**(4), 1745–1757.
- J. B. A. Arends, S. A. Patil, H. Roume and K. Rabaey, *J. CO2 Util.*, 2017, **20**, 141–149.
- E. V. LaBelle, C. W. Marshall, J. A. Gilbert and H. D. May, *PLoS One*, 2014, **9**(10), 1–10.
- I. Vassilev, P. A. Hernandez, P. Batlle-Vilanova, S. Freguia, J. O. Krömer, J. Keller, P. Ledezma and B. Viridis, *ACS Sustainable Chem. Eng.*, 2017, **6**(7), 8485–8493.
- S. Ramió-Pujol, R. Ganigué, L. Bañeras and J. Colprim, *Bioresour. Technol.*, 2015, **192**, 296–303.
- G. Wang and D. I. C. Wang, *Appl. Environ. Microbiol.*, 1984, **47**(2), 294–298.
- F. Aulenta, L. Catapano, L. Snip, M. Villano and M. Majone, *ChemSusChem*, 2012, **5**(6), 1080–1085.
- Y. Xiang, G. Liu, R. Zhang, Y. Lu and H. Luo, *Bioresour. Technol.*, 2017, **241**, 821–829.
- Z. Zaybak, B. E. Logan and J. M. Pisciotta, *Bioelectrochemistry*, 2018, **123**, 150–155.
- K. C. Wrighton, P. Agbo, F. Warnecke, K. A. Weber, E. L. Brodie, T. Z. DeSantis, P. Hugenholtz, G. L. Andersen and J. D. Coates, *ISME J.*, 2008, **2**(11), 1146–1156.
- H. Wang, L. Lu, D. Mao, Z. Huang, Y. Cui, S. Jin, Y. Zuo and Z. J. Ren, *Chemosphere*, 2019, **235**, 776–784.
- J. I. Alves, A. J. M. Stams, C. M. Plugge, M. Madalena Alves and D. Z. Sousa, *FEMS Microbiol. Ecol.*, 2013, **86**(3), 590–597.
- M. F. Alqahtani, K. P. Katuri, S. Bajracharya, Y. Yu, Z. Lai and P. E. Saikaly, *Adv. Funct. Mater.*, 2018, **28**(43), 1–8.
- M. Dopson, G. Ni and T. H. J. A. Sleutels, *FEMS Microbiol.*, 2016, **40**, 164–181.
- S. A. Patil, S. Gildemyn, D. Pant, K. Zengler, B. E. Logan and K. Rabaey, *Biotechnol. Adv.*, 2015, **33**, 736–744.

